Osteoarthritis and Cartilage 27 (2019) 314–325

Osteoarthritis and Cartilage

Coordinated existence of multiple gangliosides is required for cartilage metabolism

D. Momma †, T. Onodera † *, K. Homan †, S. Matsubara †, F. Sasazawa †, J. Furukawa †, M. Matsuoka †, T. Yamashita ‡, N. Iwasaki †

† *Faculty of Medicine and Graduate School of Medicine, Hokkaido University, Sapporo, Japan*
‡ *Laboratory of Biochemistry, Azabu University, Graduate School of Veterinary Medicine, Sagamihara, Japan*

ARTICLE INFO

Article history:
Received 30 January 2018
Accepted 14 November 2018

Keywords:
Osteoarthritis
Mice
Gangliosides
Chondrocytes
MAPKs

SUMMARY

Objective: Gangliosides, ubiquitously existing membrane components that modulate transmembrane signaling and mediate cell-to-cell and cell-to-matrix interactions, are key molecules of inflammatory and neurological disorders. However, the functions of gangliosides in the cartilage degradation process remain unclear. We investigated the functional role of gangliosides in cartilage metabolism related to osteoarthritis (OA) pathogenesis.
Design: We generated knockout (KO) mice by targeting the β1, 4-N-acetylgalactosaminyltransferase (*GalNAcT*) gene, which encodes an enzyme of major gangliosides synthesis, and the GD3 synthase (*GD3S*) gene, which encodes an enzyme of partial gangliosides synthesis. *In vivo* OA and *in vitro* cartilage degradation models were used to evaluate the effect of gangliosides on the cartilage degradation process.
Results: The *GalNAcT* and *GD3S* KO mice developed and grew normally; nevertheless, OA changes in these mice were enhanced with aging. The *GalNAcT* KO mice showed significantly enhanced OA progression compared to *GD3S* mice *in vivo*. Both *GalNAcT* and *GD3S* KO mice showed severe IL-1α–induced cartilage degradation *ex vivo*. Phosphorylation of MAPKs was enhanced in both *GalNAcT* and *GD3S* KOs after IL-1α stimulation. Gangliosides modulated by *GalNAcT* or *GD3S* rescued an increase of MMP-13 induced by IL-1α in mice lacking *GalNAcT* or *GD3S* after exogenous replenishment *in vitro*.
Conclusion: These data show that the deletion of gangliosides in mice enhanced OA development. Moreover, the gangliosides modulated by *GalNAcT* are important for cartilage metabolism, suggesting that *GalNAcT* is a potential target molecule for the development of novel OA treatments.

Introduction

Cartilage metabolism is necessary for the biomechanical and biochemical maintenance of normal cartilage. Therefore, deregulation of cartilage metabolism undoubtedly plays a crucial role in cartilage degradation causing osteoarthritis (OA). Over 70% of the world's population between the ages of 55 and 70 is affected by OA, and therapeutic options that fundamentally alter the natural course of the disease are lacking[1]. The disease costs the US economy more than $60 billion per year[2]. Since existing therapies pursue only pain palliation without preventing disease progression, a new potential disease-modifying OA drug (DMOAD) candidate is needed.

As mentioned above, the pathology of OA is characterized by a progressive degradation of articular cartilage. In healthy individuals, the homeostasis of articular cartilage is maintained primarily by chondrocytes, which are responsible for the synthesis and degradation of the extracellular matrix (ECM). However, the actual mechanisms of cartilage degradation remain unclear, despite an enormous number of gene- and protein-based studies designed to characterize the process[3–6]. Consequently, the development of OA therapies requires the identification of novel molecular targets involved in the degradation mechanism.

Gangliosides are a class of glycosphingolipids (GSLs) widely distributed on vertebrate plasma membranes and synthesized

* Address correspondence and reprint requests to: T. Onodera, Faculty of Medicine and Graduate School of Medicine, Hokkaido University, Kita 15, Nishi 7, Kita-ku, Sapporo 060-8638, Japan. Tel: 81-11-706-5935; Fax: 81-11-706-6054.
E-mail addresses: d-momma@med.hokudai.ac.jp (D. Momma), tomozou@med.hokudai.ac.jp (T. Onodera), k.houman@med.hokudai.ac.jp (K. Homan), choco1494@yahoo.co.jp (S. Matsubara), sasazawa230@gmail.com (F. Sasazawa), j_furu@med.hokudai.ac.jp (J. Furukawa), mmasatake@gmail.com (M. Matsuoka), yamashita@azabu-u.ac.jp (T. Yamashita), niwasaki@med.hokudai.ac.jp (N. Iwasaki).

https://doi.org/10.1016/j.joca.2018.11.003
1063-4584/

downstream from the ceramide (sphingosine) precursor. These molecules form clusters in membranes, where the GSLs modulate transmembrane signaling and mediate cell-to-cell and cell-to-matrix interactions[7–9]. GSLs comprise diverse types of glycolipids and are classified into several groups depending on their structure, including the o-, a- and b-series [Fig. 1(A)]. Glucosylceramide synthase (*Ugcg*), the first committed step in GSL synthesis, is a vital protein for multiple organs and cartilage; furthermore, mice with chondrocyte-specific knockout (KO) of the *Ugcg* gene have been used to demonstrate that GSLs are critical for the maintenance of chondrocyte homeostasis[10,11]. Moreover, systemic KO of GM3 synthase (*GM3S*), a downstream step in GSL synthesis, dramatically enhances cartilage degeneration without altering development, and the total ganglioside content of OA cartilage is decreased by 40%[12,13]. Considering that gangliosides are a therapeutic target has little influence on systemic conditions, specific molecules that act downstream of the ganglioside synthetic pathway are ideal candidates for a DMOAD.

Therefore, we hypothesized that the partial depletion of products downstream of *GM3S* would exacerbate OA pathogenesis. Second, we hypothesized that the severity of OA would vary according to the identity (series) and/or number of ganglioside series affected. To test these hypotheses, we employed strains of mice genetically engineered to lack β1,4-*N*-acetylgalactosaminyltransferase (*GalNAcT*) and GD3 synthase (*GD3S*) [Fig. 1(A)]. Lactosylceramide (LacCer) serves as a precursor molecule for most of the more complex ganglioside species, and mice lacking *GalNAcT* are deficient in the majority of gangliosides synthesized from LacCer[14]. In comparison, animals lacking *GD3S* are deficient in the gangliosides synthesized subsequent to GD3[15]. We analyzed here the functional roles of gangliosides in OA pathogenesis, thereby validating gangliosides as potential clinical targets in the treatment of OA. Our study shows that the absence of downstream gangliosides in mice is associated with the development of OA, and that the severity of OA depends on the number of ganglioside series affected. Gangliosides downstream of LacCer are critical molecules for cartilage homeostasis; hence, they represent potential targets for OA treatment.

Methods

Animals and generation of gene deletions

Mice with KO of the *GalNAcT* gene (*GalNAcT*$^{-/-}$) and *GD3S* gene (*GD3S*$^{-/-}$) were generated as described previously[14,15] [Fig. 1(A)]. Male adult (4-week-old and 8-week-old) and 6-week-old C57BL/6 mice were purchased from Japan SLC, Inc. (Hamamatsu, Japan). Mice were utilized after a 7-day acclimatization period following arrival[16]. The mice returned to normal behavior within 24 h after transportation. The mice were housed in a temperature- and humidity-controlled environment under 12-h light/12-h dark conditions and fed a standard rodent diet. All experiments were performed according to the protocol approved by the Institutional Animal Care and Use Committee of the Hokkaido University Faculty of Medicine and Graduate School of Medicine (Sapporo, Japan).

Isolation of chondrocytes

Chondrocytes were obtained from the knee joints of 5-day-old mice as previously described[17,18]. Briefly, cartilage specimens, obtained from femoral and tibial condyles, were treated with 0.25% trypsin (Wako, Osaka, Japan) in sterile saline for 30 min. This was followed by digestion in 0.25% collagenase (ThermoFisher Scientific, MA, USA) in culture medium consisting of Dulbecco's modified Eagle's medium (DMEM) for 4 h at 37°C in a culture bottle. Isolated primary mouse chondrocytes were cultured for 24 h in serum-free DMEM plus 10 ng/ml mouse IL-1α (Sigma, St. Louis, MO, USA) for further analysis.

Quantification of GSL-glycans in mouse chondrocytes

GSLs were recovered from mouse chondrocyte pellets by chloroform/methanol extraction. To quantify the GSL-glycomes, the glycans were released by enzymatic digestion with endoglycoceramidases I and II (EGCase I and II) derived from *Rhodococcus* species. The EGCase-digested solutions were subjected to glycoblotting as previously described[19]. Purified and labeled GSL-glycans were subjected to matrix-assisted laser desorption ionization–time-of-flight/time-of-flight mass spectrometry (MALDI-TOF/TOF MS) analysis on an Ultraflex II TOF/TOF mass spectrometer (Bruker Daltonics, MA, USA) equipped with a reflector and controlled using the FlexControl 3.0 software package (Bruker Daltonics). Peaks were detected as proton-adducted ions and annotated using the FlexAnalysis 3.0 software package with reference to the GlycoSuiteDB and SphinGOMAP databases for the structural identification of GSL-glycans.

Staining of mouse skeletons and growth plates

To observe the skeletal system, whole skeletons of wild-type (*WT*), *GalNAcT*$^{-/-}$, and *GD3S*$^{-/-}$ mice were stained with Alcian blue and alizarin red, as previously described[20,21]. To observe the growth plates, 4-week-old male mice ($n = 4$) were euthanized, and their knee joints were dissected to assess growth (weight ~15 g).

Age-associated OA model

Male mice ($n = 10$) at 4, 12, and 15 months of age (weight ~30 g) were euthanized, and their knee joints were dissected to evaluate the spontaneous development of age-associated OA[22,23].

Histologic analysis

For hematoxylin and eosin (H-E) and Safranin O (Saf-O) staining, samples were fixed in 10% buffered formalin and decalcified in 10% EDTA (pH 7.5). Each sample was dehydrated, embedded in paraffin, and sectioned into 5-μm-thick slices. Chondrocyte number and cartilage thickness were determined as previously described[22,24–26]. Three observers (DM, FS, and MM) who were blinded to the experimental groups quantified OA severity in mice using the OARSI and Mankin scoring system[26–28], and the scores obtained from the three observers were averaged.

Proteoglycan and nitric oxide (NO) release from cultured mouse cartilage explants

Ex vivo cartilage catabolism was analyzed by culturing mouse femoral head cartilage in the presence of IL-1α (Sigma)[22,29]. To assess cartilage degradation by quantification of proteoglycan release from mouse cartilage explants, the proteoglycan content in the medium and digested cartilage was measured as sulfated glycosaminoglycan using the dimethylmethylene blue assay, as described previously[22,29]. The amount of proteoglycan released from a mouse cartilage explant into the medium was quantitatively expressed as the percentage release of proteoglycan. nitric oxide (NO) was quantified based on the amount of its stable end product, nitrite, in the mouse cartilage explant culture supernatant. A Griess reagent system was used for this assay according to the recommendations of the manufacturer (Promega, Tokyo, Japan). To evaluate cartilage explant degeneration, declines in proteoglycan

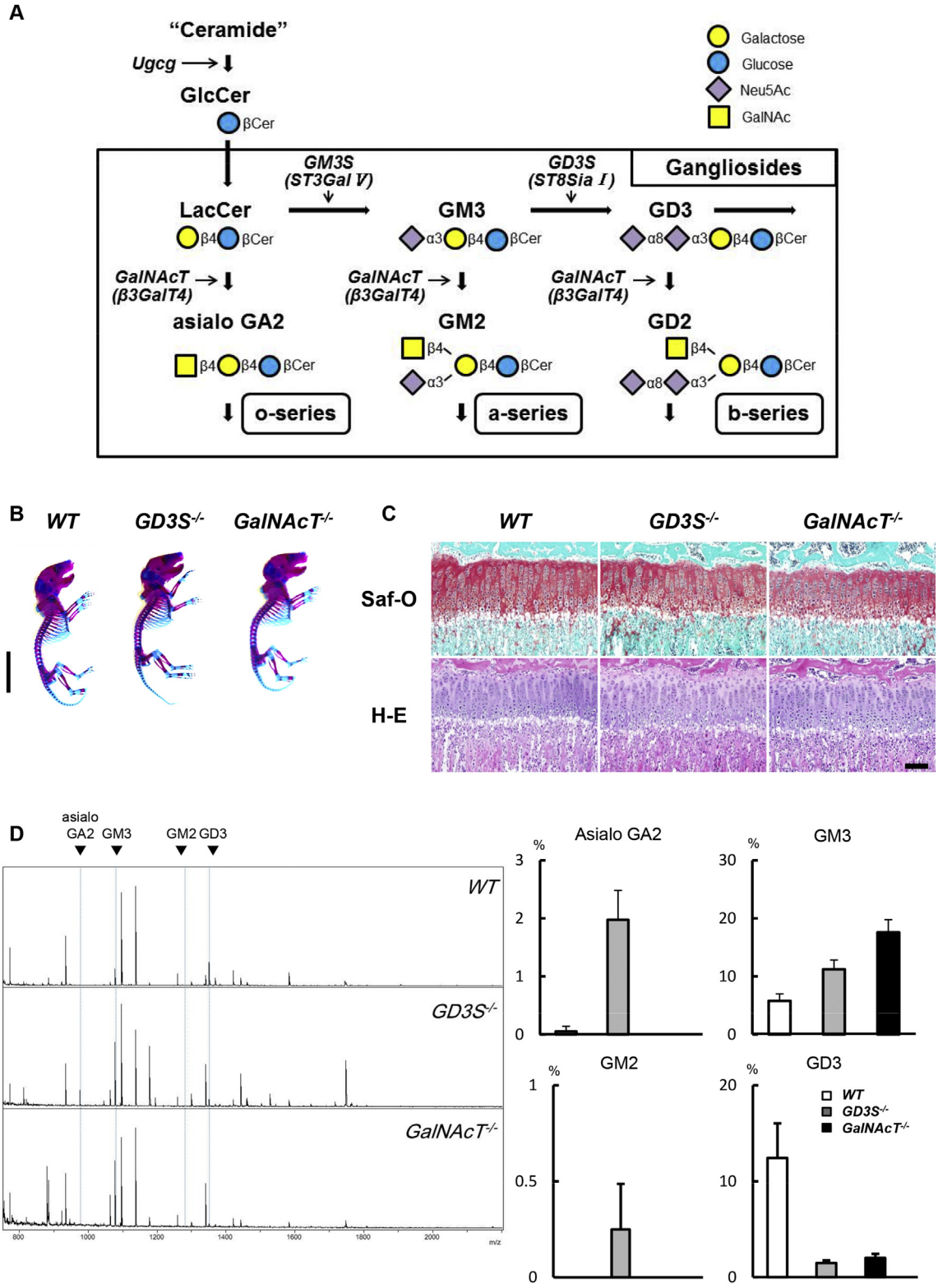

Fig. 1. Schematic of the biosynthetic pathway for gangliosides and skeletal development of *GD3S*$^{-/-}$ and *GalNAcT*$^{-/-}$ mice. A, GlcCer synthase, encoded by the *Ugcg* gene, synthesizes glucosylceramide (GlcCer) from ceramide. Gangliosides are categorized into o-, a-, and b-series. GM3 synthase (*GM3S*) is required for GSL synthesis downstream of LacCer, including the a-series and b-series. B-series gangliosides are synthesized from the common precursor molecule GD3, which is the product of GD3 synthase (GD3S, encoded by the *GD3S* gene). β1, 4-*N*-acetylgalactosaminyltransferase (*GalNAcT*) activity is required for the elaboration of the o-, a-, and b-series precursors LacCer, GM3, and GD3, respectively. B, Double staining of the whole skeleton of newborn *WT*, *GD3S*$^{-/-}$, and *GalNAcT*$^{-/-}$ mice with Alcian blue and alizarin red. Bar = 1 cm. C, Histologic findings in knee joints from 4-week-old mice. Safranin O (Saf-O) and hematoxylin and eosin (H–E) staining of tibial growth plates were performed on mice from each genotype. Growth plate width *WT*: 256.1 μm [95% CI: 236.1–276.2 μm], *GD3S*$^{-/-}$: 263.3 μm [95% CI: 243.2–283.3 μm], *GalNAcT*$^{-/-}$: 258.3 μm [95% CI: 238.2–278.3 μm]; $n = 4$. Bars = 100 μm. D, Glycoblotting in chondrocyte from 4-day-old *WT*, *GD3S*$^{-/-}$ and *GalNAcT*$^{-/-}$ mice. Values are presented as mean and 95% CI.

score were measured using the scoring system described previously[30]. In this analysis, we used four femoral heads (two mice) for each sample. We utilized eight samples (16 mice, seven male and nine female) per group.

Immunohistochemistry

Processed but unstained sections of mouse femoral head cartilage were deparaffinized, and endogenous peroxidase activity was quenched. After treatment with chondroitinase ABC (0.25 units/ml, Sigma–Aldrich, Tokyo, Japan), the sections were incubated overnight at 4°C with polyclonal antibody against the carboxyl-terminus of matrix metalloproteinase (MMP)-13 (1:200 dilution; Chemicon, Temecula, CA). The samples were then washed three times with phosphate-buffered saline (PBS) and incubated with a biotinylated secondary antibody; the primary antibody was omitted for the negative control. For semi-quantitative data, positive cells were counted in three different fields of observation at 400×magnification, and the three values were then averaged. The ratio of positive cells to total number of chondrocytes in each field was also determined. Each sample was evaluated independently by three observers who were blinded with regard to the experimental groups they were observing.

Terminal deoxynucleotidyl transferase nick-end labeling (TUNEL) assay

To investigate chondrocyte apoptosis, a TUNEL assay was performed using an *in situ* Apoptosis Detection kit according to the recommendations of the manufacturer (Takara Bio Inc., Otsu, Japan). For the negative control, the terminal transferase was omitted from the TUNEL reaction mixture. The TUNEL-positive cell ratio was calculated in the same manner as the ratio of MMP-13–positive cells.

Enzyme-linked immunosorbent assay (ELISA)

MMP-13 in the mouse chondrocyte culture supernatant was measured using an ELISA kit for mouse MMP-13 according to the manufacturer's recommendations (Uscn Life Science, Houston, TX, USA).

Quantitative real-time reverse transcriptase-PCR (RT-PCR)

Total RNA was extracted from the samples using a Qiagen RNeasy Mini kit (Qiagen, Hilden, Germany). For complementary DNA synthesis, 1.0 μg of RNA was reverse transcribed using random hexamer primers (Promega, Tokyo, Japan) and ImProm II reverse transcriptase (Promega). Real-time RT-PCR was performed using an Opticon II system (Bio-Rad, Tokyo, Japan). The reactions comprised the following steps: 95°C for 15 min, 95°C for 10 s, 60°C for 20 s and 72°C for 30 s for 40 cycles. Signals were detected using a SYBR Green qPCR Kit (Finnzymes, Yokohama, Japan) with the following gene-specific primers: Mmp-13, 5′-TTGGCCACTCCCTAGGTCTG-3' (forward) and 5′-GGTTGGGGTCTTCATCGC-3' (reverse); and Ppia, 5′-ACTTTGTCAAGCTCATTTCC-3' (forward) and 5′-TGCAGCGAACTTTATTGATG-3' (reverse) as a control housekeeping gene. The relative messenger RNA (mRNA) expression of Mmp-13 was expressed as the Ct value normalized to the Ct value of Ppia. Each reaction was run in technical triplicate in 96-well plates and biologically duplicated.

Immunoblot analysis

Chondrocytes cultured in the presence of IL-1α were prepared as described above. The medium was removed and the cells were washed twice with ice-cold PBS. Cell lysates were then extracted using PhosphoSafe Extraction Reagent (Novagen, Madison, WI) as described previously[31]. Equal amounts of protein samples were resolved on 12% SDS-PAGE gels and transferred onto polyvinylidene difluoride membranes. Proteins were probed with antibodies specific to ERK1/2, phospho-ERK1/2, JNK, phospho-JNK, p38, phospho-p38, and beta-actin (#9926, Cell Signaling Technology, MA, USA). Immunoblot intensity was analyzed using Image J software and normalized to that of β-actin. Each analysis was performed in triplicate on at least two occasions. Images were background subtracted using a rolling ball algorithm[32]. All bands were quantified values obtained by summing all bands of pP38, pJNK and pERK.

Cell culture with gangliosides

Chondrocytes from *GalNAcT*$^{-/-}$ mice were used for the analysis of Mmp-13 expression. Isolated primary mouse chondrocytes were cultured for 24 h in serum-free DMEM ±10 ng/ml mouse IL-1α with gangliosides (Elicityl, Crolles, France), including aGA2, GM2, and GD2, which were dissolved in PBS and diluted to final concentrations of 50 or 100 μM in the culture medium[33,34]. Chondrocytes from *GD3S*$^{-/-}$ mice were also used for the analysis of Mmp-13 expression. Isolated primary mouse chondrocytes were cultured for 24 h in serum-free DMEM ±10 ng/ml mouse IL-1α with gangliosides, including GD2, which were dissolved in PBS and diluted to final concentrations of 50 or 100 μM in the culture medium.

Statistical analysis

The data are expressed as means and 95% confidence intervals (CIs). The number of samples in each experimental group is shown in the figure legends. To determine significance, a 2-tailed Student's *t* test was used. *P* values less than 0.05 were considered significant. For analysis of experiments involving more than three groups, an ANOVA with the Tukey–Kramer post-hoc test was performed to determine significance. Data analysis was carried out using the statistical software JMP Pro 13.0 (SAS Institute, Cary, NC).

Results

Normal growth and development of juvenile GalNAcT$^{-/-}$ *and GD3S*$^{-/-}$ *mice*

GalNAcT$^{-/-}$ and *GD3S*$^{-/-}$ mice developed and grew normally without abnormalities in major organs and could not be distinguished from their *WT* littermates. The skeletons of newborn mice stained with Alcian blue and alizarin red did not differ in appearance among the genotypes [Fig. 1(B)]. Body weight did not differ significantly among the genotypes (data not shown). Histologic examination of the knee joints in 4-week-old mice revealed no significant differences in cartilage thickness and growth plate width among the genotypes [Fig. 1(C)]. Glycoblotting patterns were consistent with the results of each type of enzyme deficiency [Fig. 1(D)].

Depletion of gangliosides in mice expedites the development of OA with aging

Mice were followed until 15 months of age to assess the spontaneous development of OA. At 4 months of age, there were no significant differences in the development of OA in knee joints between the three genotypes [Fig. 2(A)]. Furthermore, Mankin scores showed no significant difference among the mouse genotypes (*WT*: 0.20 [95% CI: −0.05-0.45], *GD3S*$^{-/-}$: 0.10 [95% CI: −0.15-

0.35], *GalNAcT*$^{-/-}$: 0.20 [95% CI: −0.05-0.45]; $n = 10$). At 12 and 15 months of age, slight OA changes were detected in the knee joints of *WT* mice. Mild superficial cartilage erosion and a slight reduction in Safranin O staining were observed at each time point [Fig. 2(A)]. On the other hand, these OA changes were more progressed in the *GD3S*$^{-/-}$ mice than in their *WT* littermates at both 12 and 15 months of age, including joint deterioration [Fig. 2(A)]. In addition, the findings indicating OA were the most severe in the *GalNAcT*$^{-/-}$ mice, including deep erosion of the articular cartilage [Fig. 2(A)]. These histologic findings were quantitatively confirmed by the OARSI and Mankin scores [Fig. 2(B)–(D)].

Depletion of gangliosides in mice enhances IL-1α–induced cartilage degradation

The pathophysiology of OA consists primarily of the enhancement of chondrocyte apoptosis and increased production of matrix-degrading enzymes, leading to proteoglycan release and the reduction of Safranin O staining in cartilage. To analyze cartilage catabolism under *ex vivo* conditions, femoral head cartilage from the three genotypes was cultured in the absence and presence of IL-1α. IL-1α stimulation caused a significant elevation in proteoglycan release in *GD3S*$^{-/-}$ compared to *WT* explants [Fig. 3(A)]. In addition,

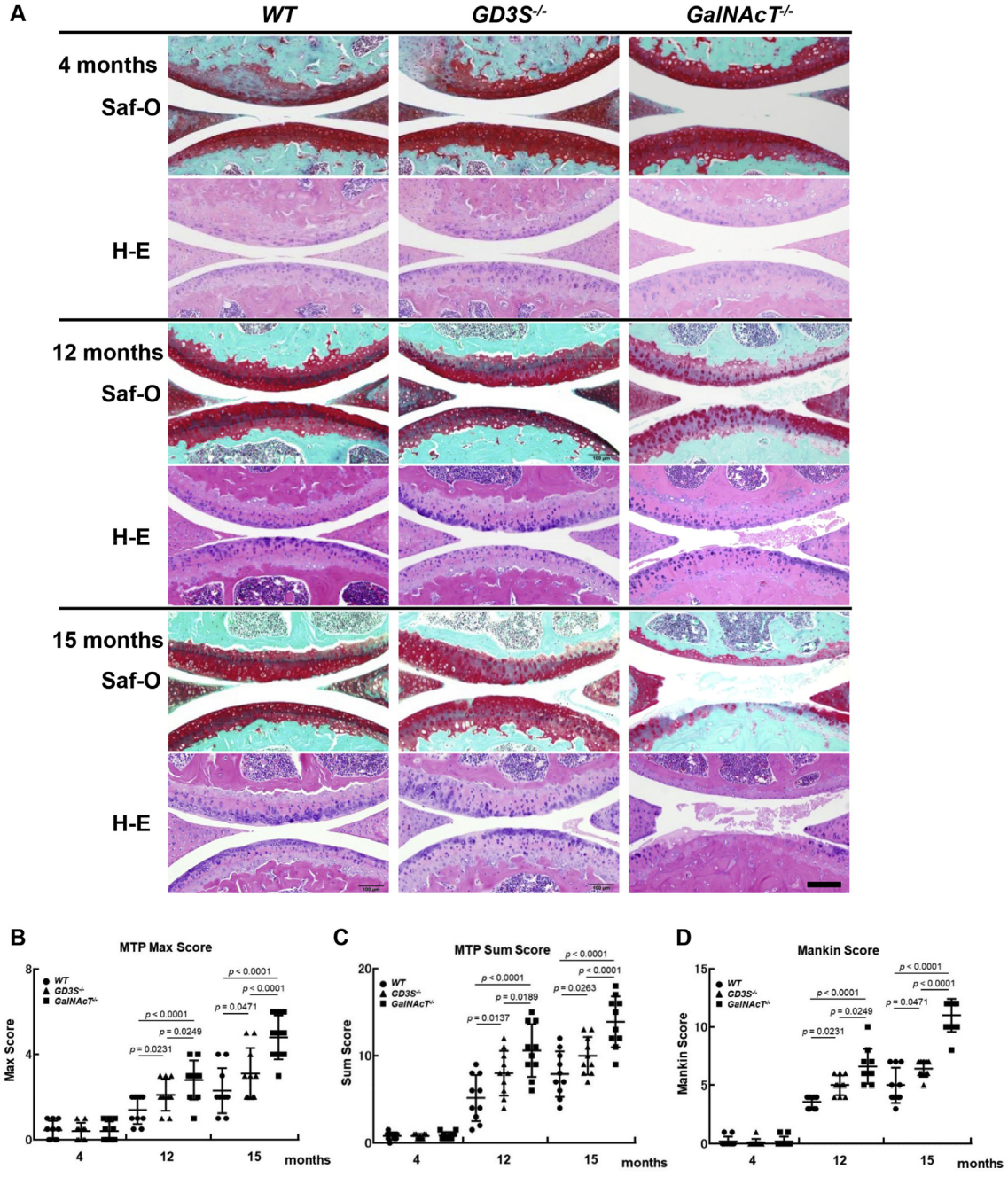

Fig. 2. Deletion of *GD3S* and *GalNAcT* accelerated cartilage degradation with age. A, Histologic assessment of age-associated OA using Safranin O (Saf-O) and hematoxylin and eosin (H–E) staining. Knee joints are shown for each mouse genotype at 4, 12, and 15 months of age. Bar = 100 μm. B, C, OARSI maximal and summed scores of the medial tibial plateau (MTP) in *WT*, *GD3S*$^{-/-}$, and *GalNAcT*$^{-/-}$ mice. OARSI maximal score at 15 months *WT*: 2.3 [95% CI: 1.6–3.0], *GD3S*$^{-/-}$: 3.1 [95% CI: 2.4–3.8], *GalNAcT*$^{-/-}$: 4.8 [95% CI: 4.0–5.6]; $n = 10$. Values are presented as mean and 95% CI. D, Mankin scores in *WT*, *GD3S*$^{-/-}$, and *GalNAcT*$^{-/-}$ mice. Values are presented as mean and 95% CI.

proteoglycan release in *GalNAcT*$^{-/-}$ explants was significantly increased compared to *GD3S*$^{-/-}$ explants [Fig. 3(A)]. We found that IL-1α–stimulated MMP-13 protein levels (in the medium) were significantly elevated in *GD3S*$^{-/-}$ compared to *WT* explants [Fig. 3(B)]. Furthermore, the MMP-13 protein levels were higher in *GalNAcT*$^{-/-}$ than *GD3S*$^{-/-}$ explants [Fig. 3(B)]. NO concentrations in the medium from *GD3S*$^{-/-}$ and *GalNAcT*$^{-/-}$ explants were higher than in *WT*. However, no significant differences were observed between the KO cartilage explants [Fig. 3(C)]. Histologic examination of the Safranin O–stained explants following IL-1α stimulation revealed no statistically significant differences among the three groups of mice [Fig. 3(D) and (G)]. MMP-13–positive cell counts revealed that the number of positive cells in *GD3S*$^{-/-}$ was significantly greater than that in *WT* after IL-1α stimulation. Also, the number of positive cells in *GalNAcT*$^{-/-}$ was significantly larger than that in *GD3S*$^{-/-}$ after IL-1α stimulation [Fig. 3(E) and (H)]. The quantification of TUNEL staining also revealed the same tendency after IL-1α stimulation [Fig. 3(F) and I].

Depletion of gangliosides upregulates Mmp-13 expression and NO release in chondrocytes cultured with IL-1α

To confirm the *in vivo* findings under *in vitro* conditions, the effect of IL-1α on Mmp-13 mRNA expression levels and NO release was measured in chondrocytes from KO and *WT* mice. Cultured chondrocytes were collected 12 and 24 h after IL-1α stimulation, and Mmp-13 mRNA levels were evaluated at each time point. The Ct values of Ppia were stable under these experimental conditions. Prior to the IL-1α–induced OA model experiment, we confirmed the expression pattern of the IL-1α receptor among the three genotypes and found that the patterns were almost identical (data not shown). We also confirmed baseline gene expression and cartilage matrix production among the three genotypes and found that the patterns were almost identical (data not shown). Similar trends were observed for the transcripts at both time points: mRNA levels in chondrocytes from *GalNAcT*$^{-/-}$ and *GD3S*$^{-/-}$ mice were significantly increased at 12 and 24 h compared to those from *WT* mice, but the levels did not significantly differ between the KO mice [Fig. 4(A) and (B)]. In addition, we found significant elevations in NO production in chondrocytes from *GalNAcT*$^{-/-}$ and *GD3S*$^{-/-}$ mice at 12 and 24 h compared to those from *WT* mice [Fig. 4(C) and (D)].

GalNAcT and GD3S invalidation enhance MAPK signaling during IL-1α stimulation

We examined the downstream signaling of IL-1α in chondrocytes to investigate the mechanism underlying the observed elevation of Mmp-13 in chondrocytes. The phosphorylation of both ERK and JNK in *GD3S*$^{-/-}$ chondrocytes was significantly upregulated to a greater degree that in *WT* chondrocytes following IL-1α stimulation [Fig. 5(A)–(C)]. IL-1α stimulation also significantly increased the phosphorylation of JNK and p38 in *GalNAcT*$^{-/-}$ chondrocytes compared to *WT* chondrocytes [Fig. 5(D)–(F)].

Gangliosides suppress IL-1α–stimulated Mmp-13 expression in GalNAcT$^{-/-}$ *and GD3S*$^{-/-}$ *chondrocytes*

To evaluate which gangliosides decrease Mmp-13 expression after IL-1α stimulation, combinations of o-, a- and b-series gangliosides were exogenously added to *GalNAcT*$^{-/-}$ chondrocytes in the presence of IL-1α stimulation for 24 h. The samples treated with all (o-, a- and b-series) gangliosides expressed significantly less Mmp-13 mRNA and NO following IL-1α stimulation compared to samples not treated with gangliosides [Fig. 6(A) and (B)]. In addition, the upregulated phosphorylation of p38 in *GalNAcT*$^{-/-}$ and that of ERK in *GD3S*$^{-/-}$ chondrocytes following IL-1α stimulation was suppressed by adding the exogenous gangliosides [Supplemental Fig. 1(A) and (B)].

B-series gangliosides were exogenously added to *GD3S*$^{-/-}$ chondrocytes in the presence of IL-1α stimulation for 24 h. The samples treated with b-series gangliosides also expressed significantly less Mmp-13 mRNA and NO following IL-1α stimulation compared with samples not treated with gangliosides [Fig. 6(C) and (D)]. A higher dose of gangliosides (100 μM) also significantly reduced the mRNA expression of Mmp-13 following IL-1α stimulation [Supplemental Fig. 1(C) and (D)].

Discussion

To identify a novel therapeutic target against OA, the authors performed a functional analysis of gangliosides in OA pathogenesis[11,13]. Mice that are homozygous null for *Ugcg*, and consequently lack all GSLs, have an embryonic lethal phenotype[10], whereas mice with a chondrocyte-specific KO of *Ugcg* progress to OA[11]. Serious side effects must be avoided when considering therapeutic targets for OA, because OA is not a fatal disease for the vast majority of afflicted patients. Moreover, systemic KO of *GM3S* dramatically aggravates cartilage degeneration without producing developmental abnormalities[13]. From these viewpoints, we speculated that the downstream gangliosides would be specifically involved in OA pathogenesis. Specific gangliosides produced downstream in the synthetic pathway represent ideal targets of DMOADs that have a low risk of producing serious side effects. The current study showed that the depletion of either a subset or the majority of gangliosides accelerated OA development in an age-associated OA model. Interestingly, younger *GalNAcT*$^{-/-}$ and *GD3S*$^{-/-}$ mice exhibited a phenotype similar to *WT* mice; however, signs of age-associated OA were more severe in the mutant mice compared to *WT* mice. These observations suggest that ganglioside deficiency produces age-associated effects on cartilage function, such as maintaining homeostasis or matrix fragility. Thus, the depletion of gangliosides deteriorates OA without producing developmental cartilage abnormalities. This indicates that downstream gangliosides are ideal target molecules for developing a novel DMOAD.

There are few studies using age-related models, despite OA being an age-related disease[35,36]. Hence, our study is consistent with OA pathogenesis from a clinical perspective. Proteoglycan deletion in the cartilage ECM is the initial step of cartilage degradation in OA[37,38]. To clarify this mechanism, we stimulated cultured mouse cartilage with IL-1α to promote proteoglycan release. Total proteoglycan released from *GalNAcT*$^{-/-}$ and *GD3S*$^{-/-}$ cartilage was significantly greater than that from *WT*. Decreased Safranin O staining of *GalNAcT*$^{-/-}$ and *GD3S*$^{-/-}$ cartilage was consistent with the observed reduction in explant proteoglycan release. These results indicate that the absence of certain gangliosides exacerbates IL-1α–induced cartilage degeneration. Furthermore, increased TUNEL and MMP-13 immunostaining in *GalNAcT*$^{-/-}$ and *GD3S*$^{-/-}$ cartilage strongly supports the theory that IL-1α stimulation accelerates cartilage degeneration by enhancing chondrocyte apoptosis and MMP-13 expression. These results were confirmed by the significant upregulation of both NO production and Mmp-13 mRNA and protein expression in *GalNAcT*$^{-/-}$ and *GD3S*$^{-/-}$ chondrocytes following IL-1α stimulation. These histological and cytological findings lead to the conclusion that deletion of gangliosides exacerbates OA and cartilage degeneration caused by proteoglycan release due to the upregulation of MMP-13 production and chondrocyte apoptosis. Thus, downstream gangliosides are profoundly involved in the early stages of OA pathogenesis.

To elucidate the mechanism of IL-1α signaling, we subsequently investigated phosphorylation of MAPK family members and found

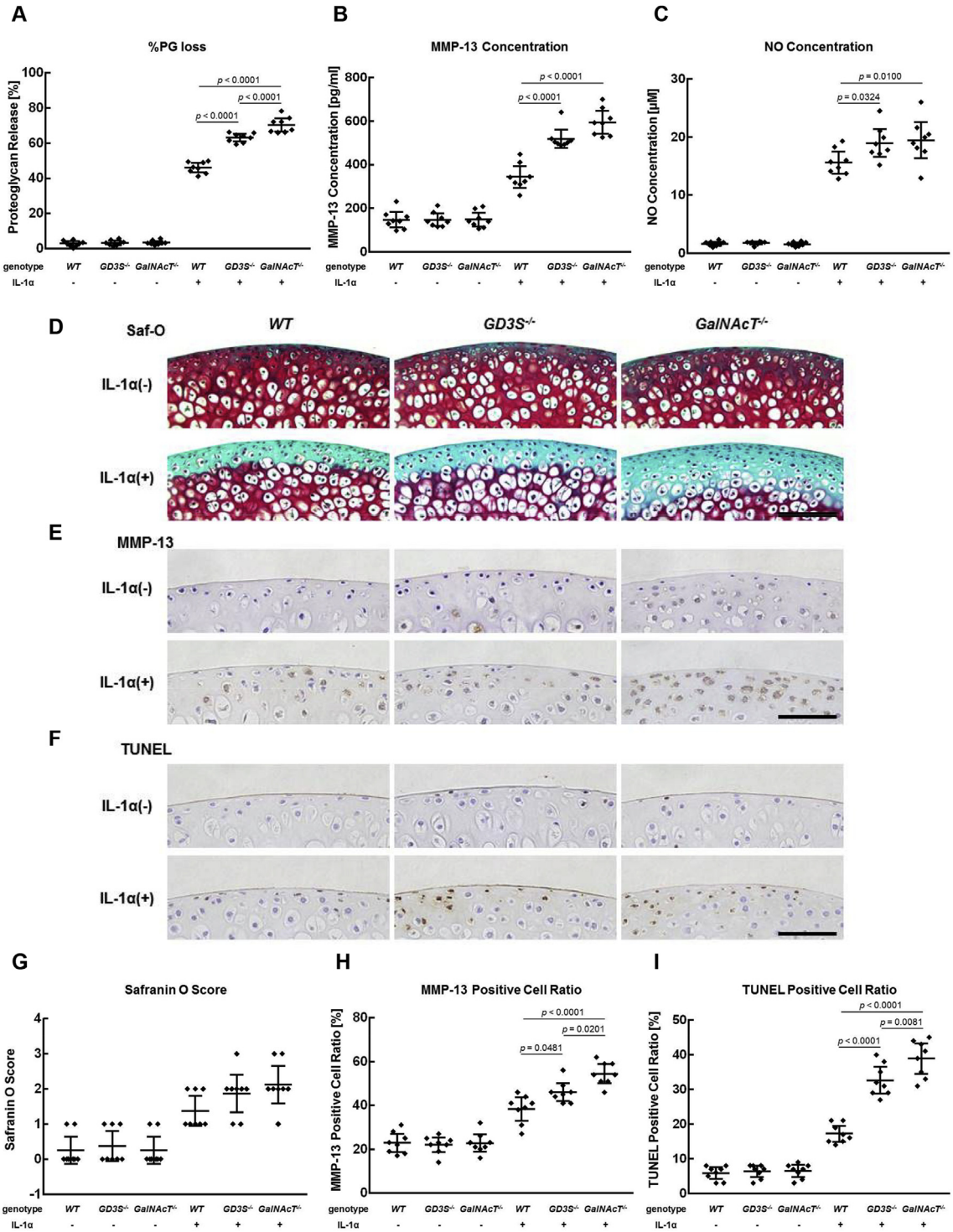

Fig. 3. Deletion of *GD3S* and *GalNAcT* accelerated Cartilage degradation induced by IL-1α stimulation. A, Proteoglycan release from cultured cartilage explants from *WT*, *GD3S*$^{-/-}$, and *GalNAcT*$^{-/-}$ mice. Proteoglycan release *WT*: 46.1% [95% CI: 44.1–48.0%], *GD3S*$^{-/-}$: 63.1% [95% CI: 61.2–65.1%], *GalNAcT*$^{-/-}$: 70.4% [95% CI: 68.6–72.4%]. B, MMP-13 concentration in media from cultured cartilage explants from *WT*, *GD3S*$^{-/-}$, and *GalNAcT*$^{-/-}$ mice. MMP-13 concentration *WT*: 344.3 pg/ml [95% CI: 305.5–383.0 pg/ml], *GD3S*$^{-/-}$: 519.3 pg/ml [95% CI: 480.5–558.0 pg/ml], *GalNAcT*$^{-/-}$: 594.4 pg/ml [95% CI: 555.7–633.1 pg/ml]. C, nitric oxide (NO) release in media from cultured cartilage explants from *WT*, *GD3S*$^{-/-}$, and *GalNAcT*$^{-/-}$ mice. NO release *WT*: 15.6 μM [95% CI: 14.1–17.1 μM], *GD3S*$^{-/-}$: 19.0 μM [95% CI: 17.4–20.5 μM], *GalNAcT*$^{-/-}$: 19.4 μM [95% CI: 17.9–21.0 μM]. D, Histologic observations in cartilage explants from *WT*, *GD3S*$^{-/-}$, and *GalNAcT*$^{-/-}$ mice cultured in the absence and presence of IL-1α and subjected to Safranin O (Saf-O) staining. Bars = 100 μm. E, MMP-13 immunostaining. F, TUNEL immunostaining. G, Cartilage degeneration score. H, MMP-13-positive cell ratio *WT*: 38.4% [95% CI: 34.8–42.0%], *GD3S*$^{-/-}$: 46.0% [95% CI: 42.4–49.6%], *GalNAcT*$^{-/-}$: 54.5% [95% CI: 50.9–58.1%]. I, TUNEL-positive cell ratio *WT*: 17.3% [95% CI: 14.8–19.7%], *GD3S*$^{-/-}$: 32.6% [95% CI: 30.2–35.1%], *GalNAcT*$^{-/-}$: 38.9% [95% CI: 36.5–41.3%]. Bars = 100 μm. Values are presented as mean and 95% CI (A-C, G-I).

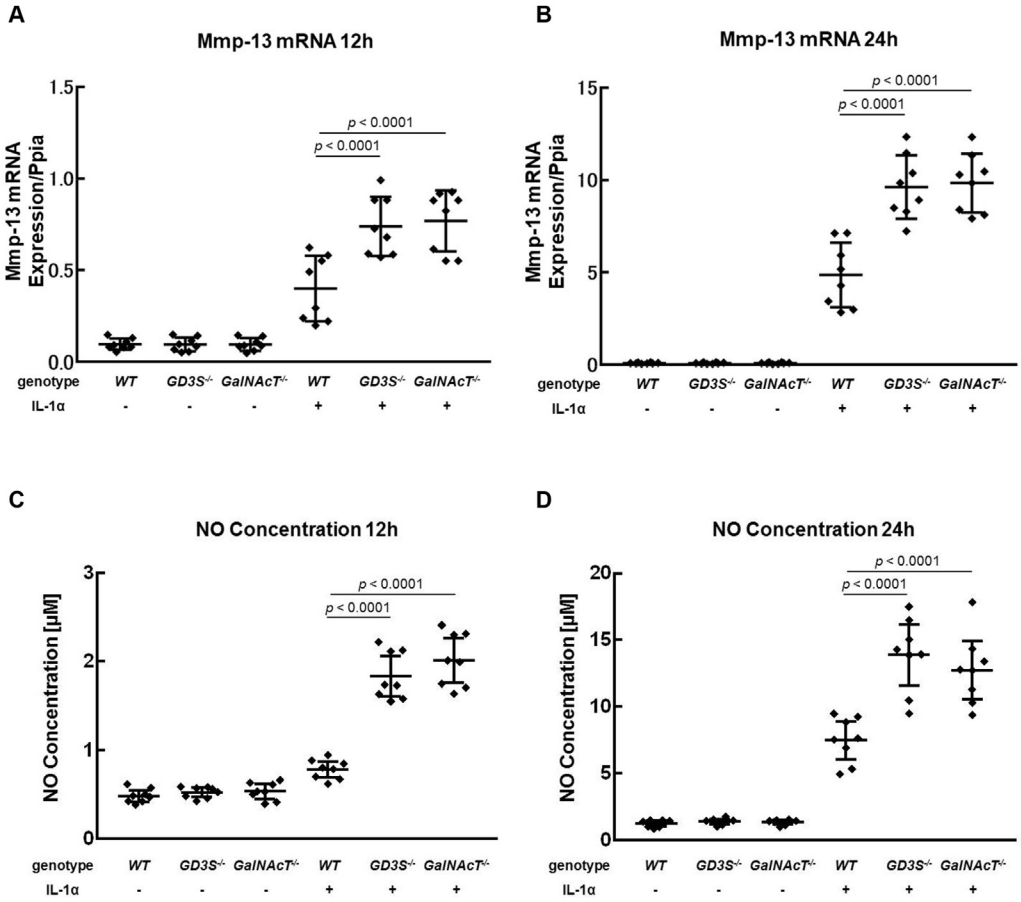

Fig. 4. Deletion of *GD3S* and *GalNAcT* accelerated expression of Mmp-13 and NO release after IL-1α stimulation *in vitro*. **A**, Expression of Mmp-13 mRNA in cultured mouse chondrocytes 12 h after IL-1α stimulation, as determined by real-time RT-PCR. *WT*: 0.27 [95%CI: 0.22–0.32], *GD3S*$^{-/-}$: 0.55 [95%CI: 0.50–0.60], *GalNAcT*$^{-/-}$: 0.53 [95%CI: 0.48–0.58]. B, Mmp-13 expression 24 h after IL-1α stimulation. *WT*: 2.99 [95%CI: 2.70–3.27], *GD3S*$^{-/-}$: 5.24 [95%CI: 4.96–5.52], *GalNAcT*$^{-/-}$: 5.10 [95%CI: 4.82–5.38]. C, Quantification of NO release in mouse chondrocyte culture supernatant 12 h after IL-1α stimulation. *WT*: 0.78 µM [95% CI: 0.65–0.91 µM], *GD3S*$^{-/-}$: 1.84 µM [95% CI: 1.71–1.97 µM], *GalNAcT*$^{-/}$: 2.01 µM [95% CI: 1.88–2.14 µM]. D, Chondrocyte NO production 24 h after IL-1α stimulation. *WT*: 7.49 µM [95% CI: 6.27–8.70 µM], *GD3S*$^{-/-}$: 13.9 µM [95% CI: 12.7–15.1 µM], *GalNAcT*$^{-/}$: 12.7 µM [95% CI: 11.5–14.0 µM]. Values are presented as mean and 95% CI.

that IL-1α stimulation significantly upregulated phosphorylation of certain MAPK family members in *GalNAcT*$^{-/-}$ and *GD3S*$^{-/-}$ mice. This suggests that gangliosides regulate the MAPK signaling pathways, causing the enhancement of Mmp-13 expression. Clinically, OA is an age-related chronic disease. Although phenotypical differences are subtle *in vitro*, we speculate that such temporary differences *in vitro* accumulate and result in apparent differences, thus inducing the characteristic pathogenesis of OA.

GalNAcT$^{-/-}$ mice exhibited dramatically exacerbated OA progression, suggesting that the lack of multiple gangliosides coordinately enhanced disease progression. On the other hand, *GD3S*$^{-/-}$ mice also exhibited increased OA severity, despite *GD3S* enabling the subsequent synthesis of a limited subset of gangliosides (b- and c-series only), indicating that the downstream products of GD3 play a specific role in OA pathogenesis. The ultimate purpose of OA research is to clarify the pathogenesis of OA and to develop treatments for this disease, such as DMOADs. To facilitate clinical application, more efficacious targets with reduced side effects are required. Although all gangliosides have the potential to contribute highly to OA pathogenesis, a few specific gangliosides may be adequate therapeutic targets for the disease. Considering that the Mankin score of *GM3S*-deficient mice at 15 months of age was 6.2 (95% CI: 4.77–7.56)[13], *GD3S* appears to be comparable to *GM3S* with respect to its role in OA pathogenesis. Each series of gangliosides is known to be related to several biological phenomena[39,40]. Specific molecules acting downstream of the ganglioside synthetic pathway may theoretically produce little influence on systemic conditions. Therefore, the gangliosides downstream of *GD3S* represent potential targets for OA treatment.

There are several limitations to this study. The current study evaluated OA in a small-animal model. A model study using larger animals would be more ideal to investigate human OA pathogenesis. In addition, synergistic and therapeutic effects of gangliosides on *in vivo* OA pathogenesis were not assessed here, and actual expression levels of each ganglioside series in OA cartilage were not determined. Further studies are needed to confirm the regulatory mechanisms and functional roles of gangliosides in OA pathogenesis and IL-1α signaling. Another limitation is that we confirmed only MAPK signaling and no proof was provided for a causal relationship. The effect of gangliosides on MAPK activation was significant but it seemed to be subtle. We speculate that signaling pathways other than MAPK may be involved. However, there were significant differences in MAPK activation among the mice. Hence, we speculate that MAPK signaling is involved in the phenotype in these KO mice. However, exploring this mechanism in WT mice remains necessary to support our current findings and conclusions. Despite these limitations, our study demonstrated that exogenous gangliosides modulated by *GalNAcT* or *GD3S* rescued an increase of Mmp-13 induced by IL-1α in *GalNAcT* or *GD3S* KO mice. Therefore, the targeting of gangliosides represents a promising new approach

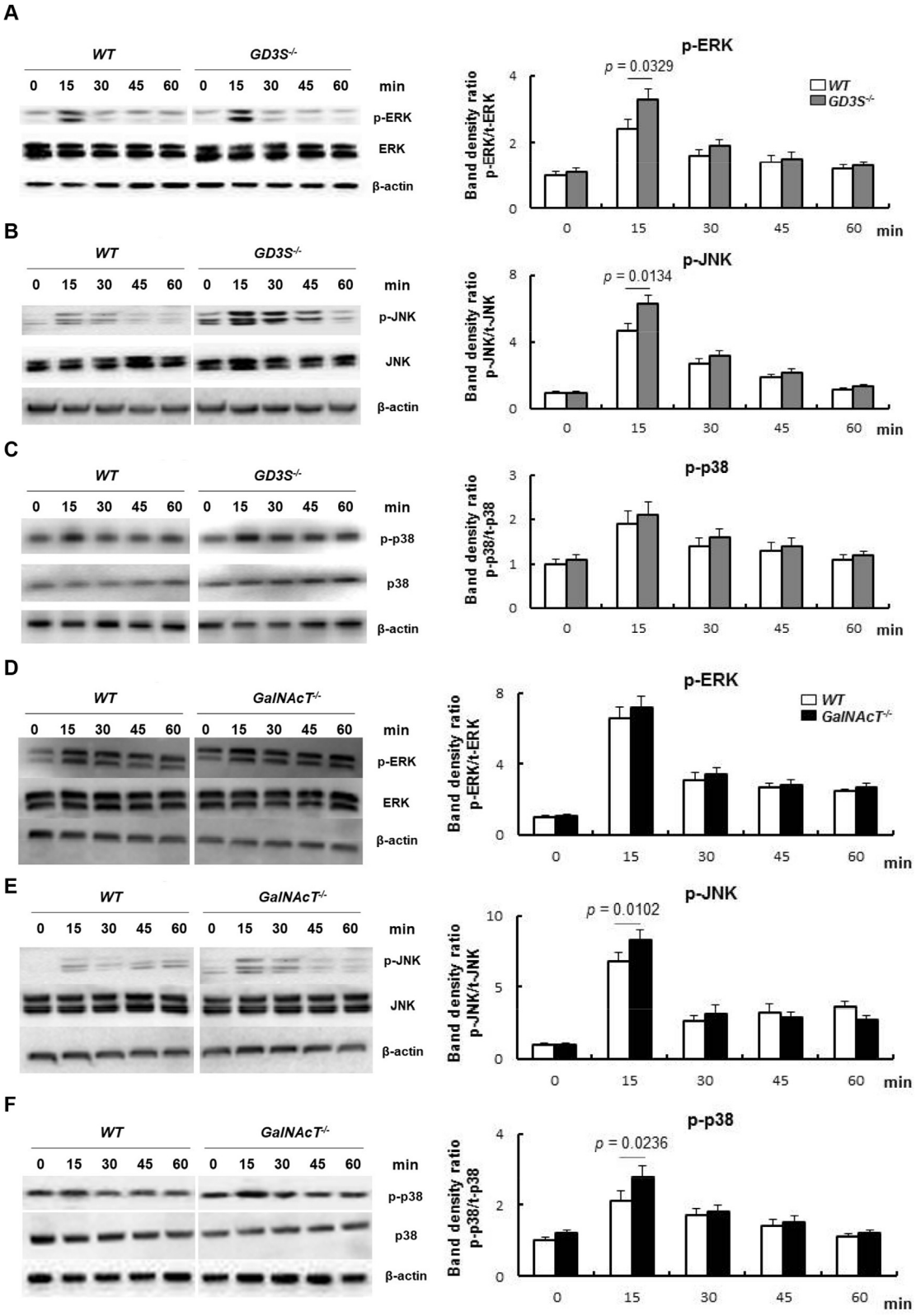

Fig. 5. Expression of MAPK family signaling molecules after IL-1α stimulation in *GD3S*$^{-/-}$ and *GalNAcT*$^{-/-}$ mouse chondrocytes. A, Expression of ERK and phospho-ERK (p-ERK) in cultured *WT* and *GD3S*$^{-/-}$ chondrocytes at 0, 15, 30, 45, and 60 min after IL-1α stimulation, as determined by immunoblot analysis. B, Expression of JNK and phospho-JNK (p-JNK), and C, p38 and phospho-p38 (p-p38). D, Expression of ERK and p-ERK in cultured *WT* and *GalNAcT*$^{-/-}$ chondrocytes at 0, 15, 30, 45, and 60 min after IL-1α stimulation, as determined by immunoblot analysis. E, Expression of JNK and p-JNK, and F, p38 and p-p38. Values are presented as mean and 95% CI.

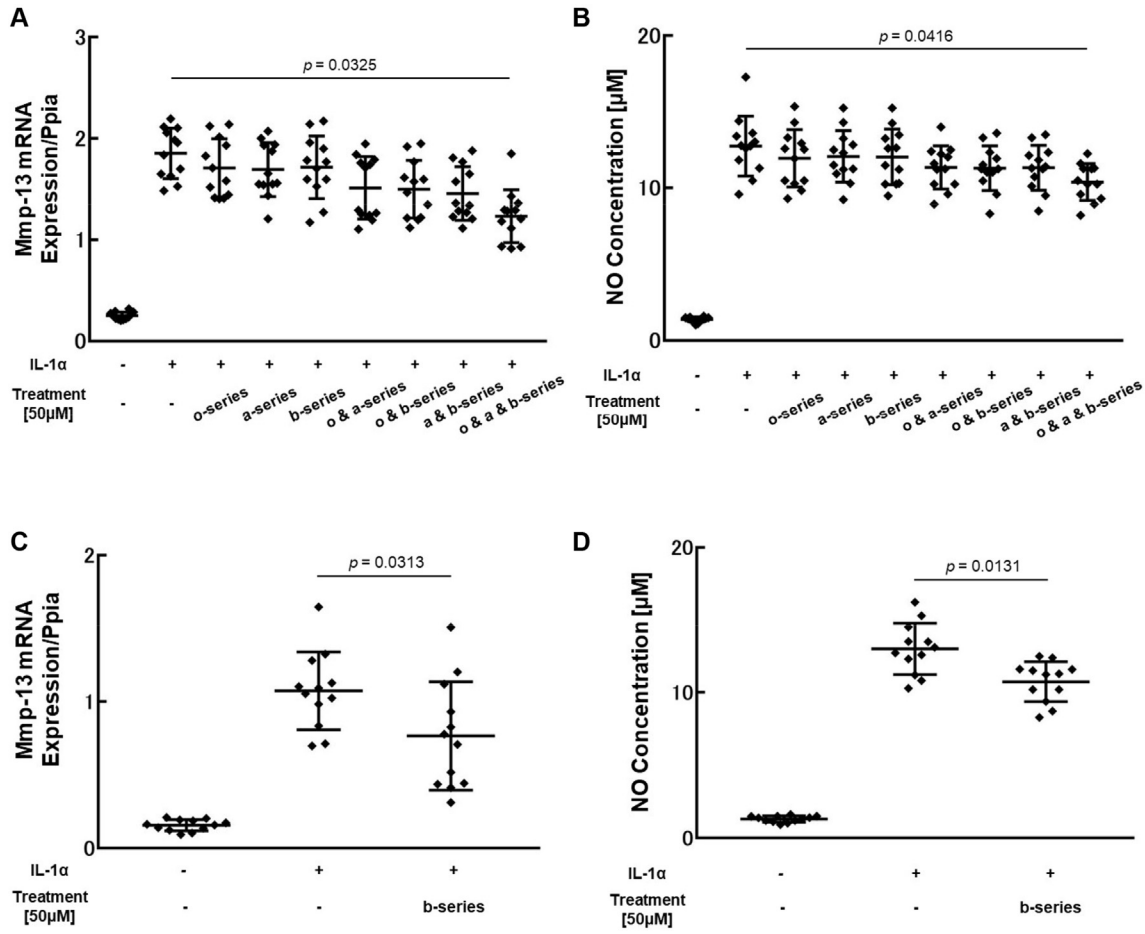

Fig. 6. Gangliosides attenuated IL-1α–stimulated Mmp-13 expression and NO release in *GalNAcT*$^{-/-}$ and *GD3S*$^{-/-}$ mouse chondrocytes. Mmp-13 mRNA expression in cultured mouse chondrocytes was determined at 24 h after IL-1α stimulation in the absence and presence of aGA2, GM2, and GD2. A, Expression of Mmp-13 mRNA, determined by real-time RT-PCR, in cultured *GalNAcT*$^{-/-}$ chondrocytes. B, Quantification of NO release in mouse chondrocyte culture supernatant. C, Expression of Mmp-13 mRNA in cultured *GD3S*$^{-/-}$ chondrocytes. D, Chondrocyte NO production. Values are presented as mean and 95% CI.

in the development of DMOADs. Our results suggest that exogenous administration of gangliosides into the joints may delay OA progression.

To the best of our knowledge, this is the first study to clarify the detailed functional roles of gangliosides in OA pathogenesis. Our mechanism-of-action study indicates that gangliosides regulate chondrocyte apoptosis and MMP-13 secretion, which contribute to the development of OA. Currently, there are no pharmacological treatments that inhibit OA progression. Although further studies will be required to clarify this mechanism, gangliosides represent potential target molecules for an effective and novel strategy for OA therapy.

Author contributions

All authors have made substantial contributions to (1), (2), and (3) below:

(1) The conception and design of the study, or acquisition of data, or analysis and interpretation of data;
(2) The drafting of the article or revising it critically for important intellectual content;
(3) Final approval of the version to be submitted.

Conflict of interest

The authors have no conflicts of interest to disclose.

Role of the funding source

This work was supported by a Challenging Exploratory Research Grant from the Japan Society for the Promotion of Science (AI24659661).

Acknowledgements

The authors thank Ms. Suyama for supporting our experiments. We also thank the Nikon Imaging Center at Hokkaido University for valuable assistance with confocal microscopy, image acquisition, and analysis.

Supplementary data

Supplementary data to this article can be found online at https://doi.org/10.1016/j.joca.2018.11.003.

References

1. Johnson K, Zhu S, Tremblay MS, Payette JN, Wang J, Bouchez LC, *et al.* A stem cell-based approach to cartilage repair. Science 2012;336:717–21.
2. Murphy L, Helmick CG. The impact of osteoarthritis in the United States: a population-health perspective. Am J Nurs 2012;112:S13–9.

3. van der Kraan PM. Osteoarthritis year 2012 in review: biology. Osteoarthritis Cartilage 2012;20:1447–50.
4. Kannu P, Bateman JF, Belluoccio D, Fosang AJ, Savarirayan R. Employing molecular genetics of chondrodysplasias to inform the study of osteoarthritis. Arthritis Rheum 2009;60:325–34.
5. Qvist P, Bay-Jensen AC, Christiansen C, Dam EB, Pastoureau P, Karsdal MA. The disease modifying osteoarthritis drug (DMOAD): is it in the horizon? Pharmacol Res 2008;58:1–7.
6. Clements KM, Price JS, Chambers MG, Visco DM, Poole AR, Mason RM. Gene deletion of either interleukin-1beta, interleukin-1beta-converting enzyme, inducible nitric oxide synthase, or stromelysin 1 accelerates the development of knee osteoarthritis in mice after surgical transection of the medial collateral ligament and partial medial meniscectomy. Arthritis Rheum 2003;48:3452–63.
7. Ichikawa S, Hirabayashi Y. Glucosylceramide synthase and glycosphingolipid synthesis. Trends Cell Biol 1998;8:198–202.
8. Hakomori SI. Structure and function of glycosphingolipids and sphingolipids: recollections and future trends. Biochim Biophys Acta 2008;1780:325–46.
9. Regina Todeschini A, Hakomori SI. Functional role of glycosphingolipids and gangliosides in control of cell adhesion, motility, and growth, through glycosynaptic microdomains. Biochim Biophys Acta 2008;1780:421–33.
10. Yamashita T, Wada R, Sasaki T, Deng C, Bierfreund U, Sandhoff K, *et al*. A vital role for glycosphingolipid synthesis during development and differentiation. Proc Natl Acad Sci U S A 1999;96:9142–7.
11. Seito N, Yamashita T, Tsukuda Y, Matsui Y, Urita A, Onodera T, *et al*. Interruption of glycosphingolipid synthesis enhances osteoarthritis development in mice. Arthritis Rheum 2012;64:2579–88.
12. David MJ, Hellio MP, Portoukalian J, Richard M, Caton J, Vignon E. Gangliosides from normal and osteoarthritic joints. J Rheumatol Suppl 1995;43:133–5.
13. Sasazawa F, Onodera T, Yamashita T, Seito N, Tsukuda Y, Fujitani N, *et al*. Depletion of gangliosides enhances cartilage degradation in mice. Osteoarthritis Cartilage 2014;22:313–22.
14. Liu Y, Wada R, Kawai H, Sango K, Deng C, Tai T, *et al*. A genetic model of substrate deprivation therapy for a glycosphingolipid storage disorder. J Clin Invest 1999;103:497–505.
15. Matsuda Y, Nara K, Watanabe Y, Saito T, Sanai Y. Chromosome mapping of the GD3 synthase gene (SIAT8) in human and mouse. Genomics 1996;32:137–9.
16. Obernier JA, Baldwin RL. Establishing an appropriate period of acclimatization following transportation of laboratory animals. ILAR J 2006;47:364–9.
17. Salvat C, Pigenet A, Humbert L, Berenbaum F, Thirion S. Immature murine articular chondrocytes in primary culture: a new tool for investigating cartilage. Osteoarthritis Cartilage 2005;13:243–9.
18. Gosset M, Berenbaum F, Thirion S, Jacques C. Primary culture and phenotyping of murine chondrocytes. Nat Protoc 2008;3:1253–60.
19. Miyaji K, Furukawa JI, Suzuki Y, Yamamoto N, Shinohara Y, Yuki N. Altered gene expression of glycosyltransferases and sialyltransferases and total amount of glycosphingolipids following herpes simplex virus infection. Carbohydr Res 2016;434:37–43.
20. Yamada T, Kawano H, Koshizuka Y, Fukuda T, Yoshimura K, Kamekura S, *et al*. Carminerin contributes to chondrocyte calcification during endochondral ossification. Nat Med 2006;12:665–70.
21. Nakamichi Y, Shukunami C, Yamada T, Aihara K, Kawano H, Sato T, *et al*. Chondromodulin I is a bone remodeling factor. Mol Cell Biol 2003;23:636–44.
22. Stoop R, van der Kraan PM, Buma P, Hollander AP, Billinghurst RC, Poole AR, *et al*. Type II collagen degradation in spontaneous osteoarthritis in C57Bl/6 and BALB/c mice. Arthritis Rheum 1999;42:2381–9.
23. Matsui Y, Iwasaki N, Kon S, Takahashi D, Morimoto J, Denhardt DT, *et al*. Accelerated development of aging-associated and instability-induced osteoarthritis in osteopontin-deficient mice. Arthritis Rheum 2009;60:2362–71.
24. Bomsta BD, Bridgewater LC, Seegmiller RE. Premature osteoarthritis in the Disproportionate micromelia (Dmm) mouse. Osteoarthritis Cartilage 2006;14:477–85.
25. Zemmyo M, Meharra EJ, Kuhn K, Creighton-Achermann L, Lotz M. Accelerated, aging-dependent development of osteoarthritis in alpha1 integrin-deficient mice. Arthritis Rheum 2003;48:2873–80.
26. Mankin HJ, Dorfman H, Lippiello L, Zarins A. Biochemical and metabolic abnormalities in articular cartilage from osteoarthritic human hips. II. Correlation of morphology with biochemical and metabolic data. J Bone Joint Surg Am 1971;53:523–37.
27. Mankin HJ. Biochemical and metabolic abnormalities in osteoarthritic human cartilage. Fed Proc 1973;32:1478–80.
28. Glasson SS, Chambers MG, Van Den Berg WB, Little CB. The OARSI histopathology initiative – recommendations for histological assessments of osteoarthritis in the mouse. Osteoarthritis Cartilage 2010;18(Suppl 3):S17–23.
29. Hashimoto S, Takahashi K, Ochs RL, Coutts RD, Amiel D, Lotz M. Nitric oxide production and apoptosis in cells of the meniscus during experimental osteoarthritis. Arthritis Rheum 1999;42:2123–31.
30. Kikuchi T, Yamada H, Shimmei M. Effect of high molecular weight hyaluronan on cartilage degeneration in a rabbit model of osteoarthritis. Osteoarthritis Cartilage 1996;4:99–110.
31. Kameda Y, Takahata M, Komatsu M, Mikuni S, Hatakeyama S, Shimizu T, *et al*. Siglec-15 regulates osteoclast differentiation by modulating RANKL-induced phosphatidylinositol 3-kinase/Akt and Erk pathways in association with signaling Adaptor DAP12. J Bone Miner Res 2013;28:2463–75.
32. Collins MA, An J, Peller D, Bowser R. Total protein is an effective loading control for cerebrospinal fluid western blots. J Neurosci Methods 2015;251:72–82.
33. Ferrari G, Batistatou A, Greene LA. Gangliosides rescue neuronal cells from death after trophic factor deprivation. J Neurosci 1993;13:1879–87.
34. Song J, Gao X, Galan JE. Structure and function of the Salmonella Typhi chimaeric A(2)B(5) typhoid toxin. Nature 2013;499:350–4.
35. Bouderlique T, Vuppalapati KK, Newton PT, Li L, Barenius B, Chagin AS. Targeted deletion of Atg5 in chondrocytes promotes age-related osteoarthritis. Ann Rheum Dis 2016;75:627–31.
36. Loeser RF, Olex AL, McNulty MA, Carlson CS, Callahan MF, Ferguson CM, *et al*. Microarray analysis reveals age-related differences in gene expression during the development of osteoarthritis in mice. Arthritis Rheum 2012;64:705–17.
37. Mizutani T, Kawabata K, Koyama Y, Takahashi M, Haga H. Regulation of cellular contractile force in response to mechanical stretch by diphosphorylation of myosin regulatory

light chain via RhoA signaling cascade. Cell Motil Cytoskelet 2009;66:389–97.
38. Chambers MG, Cox L, Chong L, Suri N, Cover P, Bayliss MT, *et al*. Matrix metalloproteinases and aggrecanases cleave aggrecan in different zones of normal cartilage but colocalize in the development of osteoarthritic lesions in STR/ort mice. Arthritis Rheum 2001;44:1455–65.
39. McDonald G, Deepak S, Miguel L, Hall CJ, Isenberg DA, Magee AI, *et al*. Normalizing glycosphingolipids restores function in CD4+ T cells from lupus patients. J Clin Invest 2014;124:712–24.
40. Ohkawa Y, Momota H, Kato A, Hashimoto N, Tsuda Y, Kotani N, *et al*. Ganglioside GD3 enhances invasiveness of gliomas by forming a complex with platelet-derived growth factor receptor alpha and yes kinase. J Biol Chem 2015;290:16043–58.